Development 138, 821-830 (2011) doi:10.1242/dev.056481

Origin of muscle satellite cells in the *Xenopus* embryo

Randall S. Daughters*, Ying Chen* and Jonathan M. W. Slack†

SUMMARY

We have studied the origin of muscle satellite cells in embryos of *Xenopus laevis*. Fate mapping at the open neural plate stage was carried out using orthotopic grafts from transgenic embryos expressing GFP. This shows that most satellite cells originate from the dorsolateral plate rather than from the paraxial mesoderm. Specification studies were made by isolation of explants from the paraxial and dorsolateral regions of neurulae and these also indicated that the satellite cell progenitors arise from the dorsolateral plate. Muscle satellite cells express Pax7, but overexpression of *Pax7* in blastomeres of whole embryos that populate the myogenic areas does not induce the formation of additional satellite cells. Moreover, a dominant-negative construct, *Pax7EnR*, does not reduce satellite cell formation. Neither *Pax7* nor other myogenic transcription factor genes will induce satellite cell formation in animal caps treated with FGF. However, BMP RNA or protein will do so, both for FGF-treated animal caps and for paraxial neurula explants. Conversely, the induction of *Noggin* in dorsolateral explants from *HGEM-Noggin* transgenic neurulae will block formation of satellite cells, showing that BMP signaling is required in vivo for satellite cell formation. We conclude that satellite cell progenitors are initially specified in the dorsal part of the lateral plate mesoderm and later become incorporated into the myotomes. The initial specification occurs at the neurula stage and depends on the ventral-to-dorsal BMP gradient in the early embryo.

KEY WORDS: *Xenopus*, Muscle satellite cell, Myogenesis, BMP, Pax7

INTRODUCTION

Muscle satellite cells are the stem cells of skeletal muscle (Hawke and Garry, 2001; Morgan and Partridge, 2003; Chargé and Rudnicki, 2004). They proliferate and contribute to new muscle formation during the growth of the animal, and then become quiescent in the adult. They are small cells lying beneath the basement membrane surrounding the multinucleate muscle fibers. Skeletal muscle does not show continuous cell turnover in the adult organism but following muscle damage satellite cells become reactivated. They are then released from the muscle fibers, divide, start to express myogenic transcription factors and become myoblasts. These may develop into myofibers or fuse with pre-existing fibers. Following reactivation, the satellite cells also undergo renewal divisions to maintain a population of undifferentiated satellite cells, although the cell number tends to fall with age (Kuang et al., 2008).

The biology of satellite cells in the adult has been well studied, but their origin in the embryo remains unclear. Previous studies in the mouse and chick embryo indicated that satellite cells originate from the somites and in particular from a *Pax3/7*-positive population of cells located in the central region of the dermomyotome of the somite (Armand et al., 1983; Gros et al., 2005; Relaix et al., 2005). But these studies did not indicate the origin of the satellite cells prior to somitogenesis, nor whether they come from the same or different region as the myoblasts that form the primary and secondary myofibers. Studies in the zebrafish indicate that at least some satellite cells come from anterior border cells within the somites, that later form a layer on the outer surface of the myotomes (Hollway et al., 2007). Although an origin from the somites is now thought most likely, some other studies had previously suggested an origin from quite distinct embryonic structures such as the dorsal aorta (De Angelis et al., 1999).

The *Xenopus* embryo offers an opportunity to investigate this problem. Unlike the mouse or chick, the neurula stage embryo is easily accessible and is well suited to microsurgical experiments. Muscle satellite cells certainly exist in *Xenopus*. Indeed they were first discovered in another frog species (Mauro, 1961). Our previous work on regeneration of tail muscle indicated that the *Xenopus* tail muscle contains abundant Pax7-positive cells and that these cells are able to regenerate the tail muscle following tail amputation (Chen et al., 2006). Like mammalian satellite cells, these Pax7-positive cells are small, with limited cytoplasm, and lie beneath the basement membrane of the muscle fibers. In the tadpole, which is growing in size, these cells are frequently in cycle, as shown by labeling with BrdU, whereas the myofiber nuclei are not. Although the *Xenopus* cells do not display all the molecular markers that have been associated with satellite cells in the mouse, by virtue of their Pax7 expression, morphology, location and behavior during muscle regeneration, they may be considered to be the exact equivalent of satellite cells in mammals. Satellite cells have also been examined in urodele amphibians and seem similar except that they are completely surrounded by the myofiber basement membrane (Morrison et al., 2006).

Our previous work on the cell lineage of the regenerating tail suggested that the paraxial mesoderm of the open neural plate neurula may contain few if any satellite cell precursors (Gargioli and Slack, 2004). The present study was aimed at investigating where the satellite cells do come from in the embryo and what factors lead to their formation.

We show here that a satellite cell precursor zone may be identified before the formation of the somites. It does not lie in the paraxial mesoderm, normally considered to be equivalent to the presomite plate, but in the adjacent dorsal part of the lateral plate. We show that the formation of satellite cells is promoted by BMP

Stem Cell Institute, University of Minnesota, MTRF, 2001 6th Street SE, Minneapolis, MN 55455, USA.

*These authors contributed equally to this work
†Author for correspondence (slack017@umn.edu)

Accepted 4 December 2010

signaling. A ventral-to-dorsal gradient of BMP activity is a general feature of early vertebrate development. In *Xenopus*, it is set up at the beginning of gastrulation and is based on a widespread expression of BMP genes in the ventrolateral sector of the embryo, coupled with a localized secretion of BMP inhibitors (Chordin and Noggin) from the organizer region. It is well recognized that the BMP gradient controls mesoderm patterning during gastrulation (Hemmati-Brivanlou and Thomsen, 1995; Dosch et al., 1997; De Robertis, 2009) and we show here, at least with regard to satellite cell formation, that this gradient remains active into the neurula stages. We further show that the transcription factor Pax7 itself, although it is needed for satellite cell function in regeneration (Chen et al., 2006), is not involved in the initial formation of satellite cells.

MATERIALS AND METHODS

Grafts and explants

For fate mapping of the mesoderm, transgenics were prepared and grafts were performed, as described previously (Gargioli and Slack, 2004). Hosts were cultured until stage 48/49.

Explants from neurulae were microdissected from stage 13-14 embryos corresponding to paraxial mesoderm or dorsolateral mesoderm, but including all three germ layers. Explants were individually cultured in 24-well plates in 0.5×NAM for 4 days. BMP treatment was 100 ng/ml rBMP4 (R&D Systems) for 24 hours followed by 3 days in 0.5×NAM.

For inhibition of BMP by Noggin, explants were dissected from *HGEM-Noggin* transgenic embryos (Beck et al., 2006), placed in 0.5×NAM plus or minus rBMP4 (100 ng/ml) and 4 hours later subjected to a heat shock (34°C for 15 minutes). Explants were cultured at room temperature for 24 hours, subjected to a second heat shock, and cultured for an additional 3 days in 0.5×NAM at room temperature.

Animal caps

Embryo culture and bFGF (50 ng/ml, R&D Systems) treatment of animal cap explants were carried out as described previously (Isaacs et al., 1994). Before dissection of animal caps, synthesized mRNA of candidate factors were individually injected in a volume of 9.2 nl into the animal pole region of both blastomeres at the two-cell stage.

To detect gene expression in animal cap explants, RT-PCR was performed on RNA extracted from five animal caps at day 5. One microgram of RNA was reverse transcribed and 1/20th of the cDNA reaction volume (1 μl) was amplified 30 cycles by PCR. Primers are listed in Table S1 in the supplementary material.

In situ hybridization and immunohistochemistry

Whole-mount in situ hybridization and immunostaining were performed as described previously (Gargioli and Slack, 2004; Chen et al., 2006). For whole-mount immunofluorescence of explants and tadpole tails, tissue was fixed using a variable pH paraformaldehyde fixative procedure modified from Daughters et al. (Daughters et al., 2001). Briefly, tissue was incubated at room temperature for 5 minutes in 2% PFA (pH 6.5), followed by a 1 hour incubation in 2% PFA (pH 8.5) at room temperature. Primary antibodies used in the study were Pax7 (DSHB), NCAM (Chemicon), GFP (Abcam), pSmad1 (Cell Signaling) and Myosin (made in the J.M.W.S. laboratory).

Stained tissue was visualized on an inverted confocal microscope and analyzed using FV1000 software (Olympus). Photomicrographs are composite images of 5 μm optical slices through the tissue compressed along the *z*-axis and represent approximately 150 μm depth. Images were further processed using Photoshop (Adobe Systems).

RESULTS

Fate mapping of satellite cell progenitors in the neurula

To identify the origin of muscle satellite cells in the neurula, we carried out a fate-mapping study of the trunk/tail mesoderm of stage 13/14 *Xenopus* embryos. This was done by making orthotopic grafts of small pieces of tissue from *CMV-GFP* transgenic donors to wild-type host embryos, allowing them to develop to a stage at which satellite cells have differentiated (stage 48), and then counting the satellite cells within the area of the graft. Open neural plate neurulae (stage 13-14) were used for transplantation because this is before somite formation and at this stage the mesoderm is easily isolated free from the other germ layers. Furthermore, the position of the newly formed open neural folds provides an anatomical reference for the underlying tissue regions that were grafted. We carried out orthotopic grafts of three regions of mesoderm in the prospective trunk as shown in Fig. 1A,B: paraxial, dorsolateral and ventrolateral. The paraxial tissue is the thick mesoderm lying beneath the neural plate, while the dorsolateral and ventrolateral regions are of approximately the same breadth (100 μm) but lesser thickness. The dorsolateral region expresses many lateral plate markers, although expression of some somite markers also overlaps into this region (Pollet et al., 2005). All three regions populate much of the tail, as well as the trunk (Tucker and Slack, 1995). We raised the host embryos to stage 48 tadpoles, and checked the position of the graft by GFP expression in the whole tadpole before preparing transverse sections. The GFP-positive domain resulting from each type of graft was sectioned and stained with antibodies to GFP and to Pax7. The number of labeled myofibers and satellite cells was counted within a standard volume (10×10 μm sections, area 120 μm^2). Pax7 staining was used, together with cell morphology, to

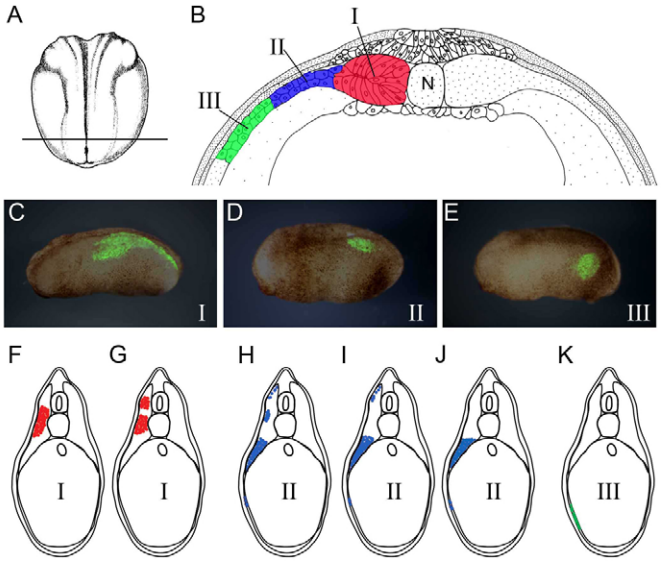

Fig. 1. Fate mapping by orthotopic graft. (**A**,**B**). Location of paraxial, dorsolateral and ventrolateral regions of mesoderm used for orthotopic grafts. (A) Dorsal view of a stage 13 embryo. Anterior is upwards. The line indicates the position of the cross-section shown in B. (B) The mesoderm regions indicated by I, II and III stand for the paraxial, dorsolateral and ventrolateral mesoderm, respectively. N, notochord. (**C-E**) Typical labeling patterns for the three types of graft, viewed by GFP fluorescence. (**F-K**) Labeling patterns of typical individual embryos projected onto standard transverse sections of stage 32 embryos. The red in F and G shows two typical labeling distributions of paraxial mesoderm grafts. The blue in H-J shows three typical labeling pattern of dorsolateral mesoderm grafts. (K) Labeling of ventrolateral mesoderm always goes to the body wall or the gut wall, indicated in green.

Table 1. Orthotopic grafts from *GFP* transgenics to wild-type hosts

Graft	Paraxial		Dorsolateral	
Number of tadpoles	8		11	
Cell type	Myofibers	Satellite cells	Myofibers	Satellite cells
Mean labeled cell count per tadpole	175 (13.5)	7.7 (1.3)	99 (9.8)	25.5 (2.5)
Percentage of cells labeled in donors	96.3	50.7	93.6	47.9
Corrected cell count	182	15.2	105.7	53.2
Total number of this cell type/tadpole	255 (10.5)	91.2 (4.0)	280 (11.1)	104 (8.4)
Percentage of this cell type in the counted volume that is derived from the graft	71	17	38	51

Paraxial and dorsolateral refer to the regions of mesoderm grafted to an orthotopic site in the host. Operations were carried out at early neurula stage, and the cell counts were made at tadpole stage 48. Cells were counted in a 120 μm^2 counting area on 10 sections of 10 μm thickness for each tadpole. The percentage of labeled cells in donors refers to counts made in the same volume of the donors used for these hosts, and also reared to stage 48. The corrected cell count allows for the fact that GFP is not visible in all donor-derived cells, and this correction also incorporates the effect of cell fusion in the formation of multinucleate myofibers. The total number counts refer to the total myofibers or satellite cells in the counted volume. Figures in brackets are standard errors.

identify satellite cells. There are also some Pax7-positive cells in the central nervous system at this stage (Chen et al., 2006) but these cannot be confused with muscle satellite cells.

The ventrolateral grafts never contributed any cells to the myotomes, but the paraxial and dorsolateral grafts both did so (Table 1). The gross distribution of labeled cells is shown for some typical closed neurulae (whole mounts showing GFP, stage 20-25, Fig. 1C-E), and for cross sections of typical tailbud stages at trunk level (drawings, stage 32, Fig. 1F-K). Cells from the paraxial region populate the central part of the mature somites. Cells from the dorsolateral region accounts for about one third of cells in the somites. They are always found in the ventral region and in 67% cases also in the dorsal region. This behavior is not surprising in view of the known dorsal convergence of mesoderm in the neurula and post-neurula stages (Hamilton, 1969). The gross picture remains the same at the later stage used for the analysis of satellite cell formation (tadpole stage 48). Among the three regions of mesoderm grafted, we found that only cells from paraxial and dorsolateral grafts end up within the myotomal skeletal muscle. The ventrolateral grafts populate entirely the connective tissue of the body wall or the gut wall (100%, n=15). For this reason, we excluded the ventrolateral region from further consideration.

The *GFP* construct used includes a nuclear localization sequence and the protein is enriched in nuclei. However, it is also present in the cytoplasm and so it is easy to identify labeled myofibers in transverse sections not containing a myonucleus. Although the transgenic embryos should theoretically express GFP in all cells, when sections were examined we found that on average only 92% of myofibers and 63% of satellite cells were positive for GFP under the conditions of our analysis (n=10, see Fig. S1 in the supplementary material). The percentage of labeled myofibers may be expected to be higher than other cell types because cell fusion means that not all nuclei in a fiber need be transgenic for the fiber to be green. Because each transgenic tadpole is a founder animal, we took the precaution of keeping all the donor embryos and raised them to the same stage as the corresponding hosts. Donors tend to have some defects but can usually survive to stage 48 and so each one was sectioned and the percentage of GFP-positive cells recorded for the myofibers and the satellite cells. In this subset of donors (n=19), the figures were 95% for myofibers and 49% for satellite cells, and there was no difference between the groups of donors used to provide the paraxial and dorsolateral grafts. These donor counts were used to correct the numbers of GFP-positive cells found in the corresponding hosts, and convert them to numbers of graft-derived cells. A total of 19 host tadpoles were counted and the counts were of a 120 μm^2 area across 10 sections spanning the region containing GFP-labeled cells. The results are expressed in terms of the number of cells of each of the two types formed from the graft within the standard volume that was counted. The collected data are shown in Table 1 and typical specimens in Fig. 2B,C. The results show that the paraxial mesoderm gave rise to a high proportion (71%) of myofibers but few (17%) satellite cells derived from the graft, whereas the dorsolateral region gave rise to many satellite cells (51%) but fewer myofibers (38%) derived from the graft. The precision of this type of study is necessarily limited by small dissection errors and small variations in healing of grafts into position. So the spatial resolution cannot be very high. However, the result clearly indicates that in normal development the satellite cell precursors originate from a more lateral level than the myofibers, most coming from outside the thickened region of paraxial mesoderm.

Specification of satellite cell progenitors

The fate-mapping result shows only the origin of the satellite cells in normal development and does not give any information about whether their progenitors are already specified at the time of grafting. This was investigated by culturing explants of tissue from early neurulae (stage 13-14) for 5 days until sibling controls had

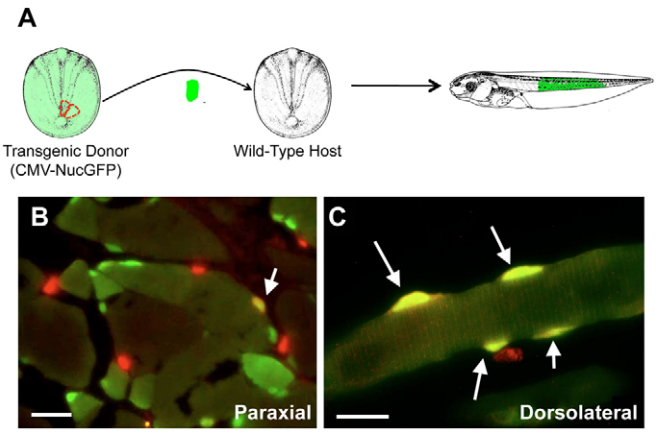

Fig. 2. Origin of satellite cells in neurula stage mesoderm. (**A**) Orthotopic grafting from a *GFP* transgenic donor into wild-type host. (**B**,**C**) Immunofluorescent images of tail muscle of host tadpoles demonstrating Pax7-labeled satellite cells (red) colocalized with GFP. Grafts of paraxial mesoderm labeled few if any satellite cells (arrow in B), while grafts of dorsolateral mesoderm labeled significantly more satellite cells (arrows in C).

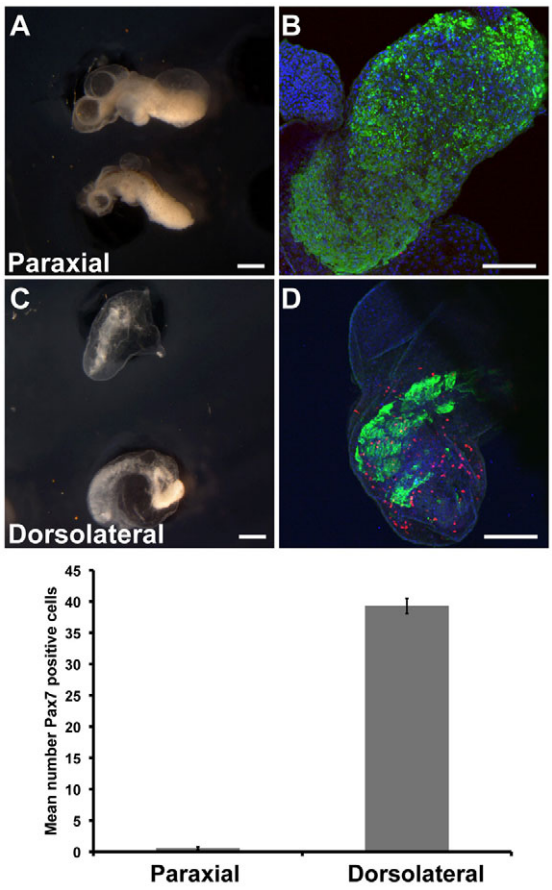

Fig. 3. Specification of Pax7-positive cells in neurula explants. (**A**) Paraxial explants. (**B**) Confocal view of paraxial explant immunostained for Myosin (green) and Pax7 (red). There are many myofibers but almost no Pax7-positive cells. (**C**) Dorsolateral explants. (**D**) Confocal view of dorsolateral explant immunostained for Myosin (green) and Pax7 (red). There are many Pax7-positive cells. DAPI staining (blue) was used to identify total nuclei. Scale bars: 200 μm. Bar chart shows the mean number of Pax7-positive cells counted per explant. Data are mean ± s.e.m. *n*=12 for each explant type.

reached stage 48. These explants were full thickness, containing the overlying ectoderm as well as the mesoderm of the appropriate level, and results are shown in Fig. 3.

This showed two things very clearly. First, Pax7-positive cells do develop in the dorsolateral explants (mean 39.3 cells/explant). In some cases (four out of 12) they did so in the complete absence of myofibers, indicating that they can differentiate autonomously and do not require any interaction with developing myofibers. Second, virtually no Pax7-positive cells differentiated in the paraxial explants (mean 0.56 cells/explant). The specification study shows a sharper difference between the paraxial and dorsolateral levels than the fate map study. This may be because the fate map study has a larger variance due to the grafting procedure, or because the environment in the two types of explants reinforce the initial difference in progenitor cell representation, or both. Because the position of satellite cells under the muscle fiber basement membrane cannot be defined if they are not associated with fibers, for this and other explant experiments, we refer to 'Pax7-positive cells' rather than 'satellite cells'. However, we believe that they are in fact satellite cells.

Role of Pax7 in initial specification of satellite cells

Because of the well established importance of Pax7 for satellite cell function, we investigated whether Pax7 itself is involved in the initial formation of satellite cells by overexpressing either *Pax7* or a dominant-negative construct, *Pax7EnR*. The activity of Pax7EnR as an inhibitor of Pax7 was demonstrated in our previous publication (Chen et al., 2006). To limit damage to other parts of the embryo, these overexpression experiments were carried out by injection of mRNA into single blastomeres at the 32-cell stage. According to the fate map (Dale and Slack, 1987), blastomere C3 projects to the paraxial region of the trunk and blastomere C4 to the lateral plate of the trunk. The domains filled by these blastomeres at trunk level thus approximate to the regions studied in our microsurgical experiments, with C3 roughly corresponding to the paraxial mesoderm and C4 to the dorsolateral and ventrolateral mesoderm (see Fig. S2 and Table S2 in the supplementary material).

Following injection of *Pax7* mRNA, there was an induction of ectopic *Pax3* (C3 or C4 injection) and *Myf5* (C3 injection only) (Fig. 4; see Table S3 in the supplementary material), indicating that the injected RNA is biologically active. But the number and position of muscle fibers remained normal.

To examine the effects on satellite cell formation, we examined sections of the C3-injected tadpoles at stage 45, double immunostained with Pax7 and NCAM antibodies. The reason for using NCAM as well as Pax7 is because there might be residual Pax7 protein present resulting from the *Pax7* RNA injection. Ten specimens of each kind of injection were used, with five sections counted from each. This showed no increase in the number of satellite cells on the injected side (Fig. 4J). The same was true of the C4-injected embryos. There was also no effect on the number of satellite cells following injection of 100 pg *Pax7EnR* mRNA into the C4 blastomere (Fig. 4J).

The overexpression experiment shows that Pax7, either alone or together with the induced Pax3, is not sufficient to specify either myogenic or satellite lineages. The dominant-negative experiment shows, in addition, that Pax7 is not required for satellite cell formation. There is no doubt that Pax7 is required for satellite cell function at later stages, but by then the *Pax7EnR* RNA will have degraded and will no longer be active.

Factors affecting satellite cell formation

In order to investigate what factors do affect satellite cell formation, we adapted the animal cap assay. Isolated animal caps do not form either myofibers or satellite cells. However, significant muscle masses are induced following treatment with fibroblast growth factors (Slack et al., 1987). Interestingly, we found that such induced caps do not generate Pax7-positive cells. Although the intact embryo contains some Pax7- positive neurons by stage 48, our animal cap explants also did not produce any neural tissue in these experiments.

For testing factors, two-cell stage embryos were injected with either control (*GFP*) or candidate factor mRNA. Animal caps were removed at blastula stage 8-9, induced to form mesoderm with FGF2 and maintained in culture medium for 5 days to allow time for the development of Pax7-positive cells. In response to mRNA encoding early myogenic regulatory factors, including Pax3, Pax7 and Myf5, there was no expression of endogenous *Pax7* or formation of Pax7-positive cells (see Table S4 in the supplementary material). This confirmed the results from the whole embryo experiments presented above. Similar results were observed for

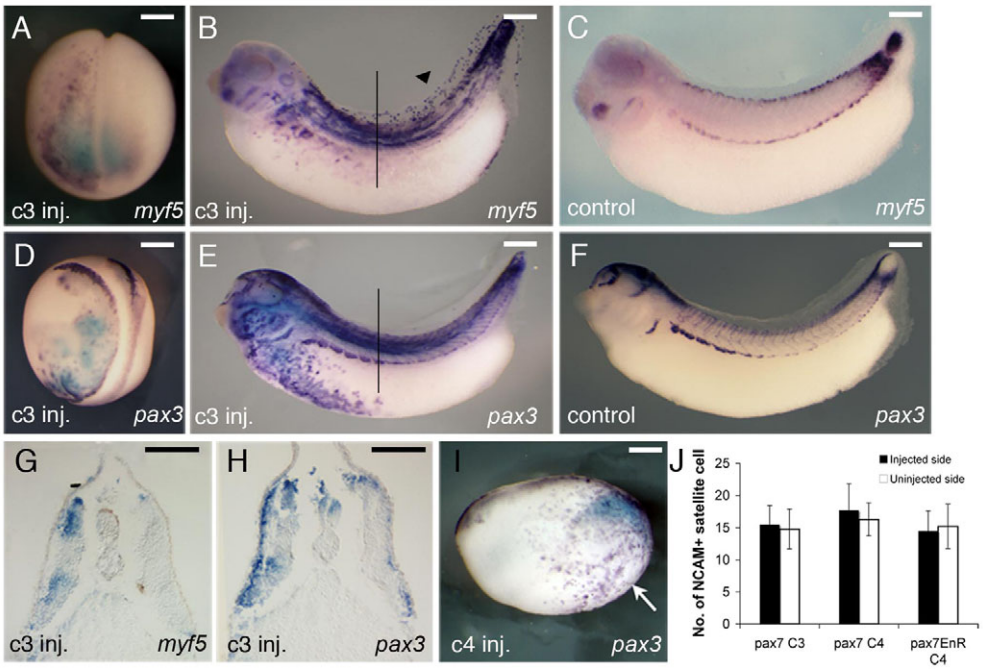

Fig. 4. *Pax7* mRNA injection induces ectopic expression of *Myf5* and *Pax3*. *Xenopus Pax7* mRNA (1 ng) was injected into blastomere C3 of the left side at 32-cell stage. (**A**,**B**,**G**) Expression of *Myf5*. (**C**) Control embryo showing normal *Myf5* at stage 34. (**D**,**E**,**H**) Expression of *Pax3*. (**F**) Control embryo showing normal *Pax3* at stage 34. (**I**) Expression of *Pax3* mRNA in embryo injected with *Pax7* mRNA in C4 blastomere at 32-cell stage. Arrow indicates ectopic *Pax3* expression. (**J**) Effect on satellite cell numbers of overexpression of *Pax7* or *Pax7EnR*. There is no significant difference between the number of satellite cells on the injected and uninjected side. Each count represents five sections from 10 embryos. Results are mean ± s.e.m. The black lines in B and F indicate the position of sections in D and H, respectively. The black arrowhead in B shows the expression of *Myf5* in fins. Scale bars: 100 μm.

factors affecting the Notch and Wnt pathways, which are known to regulate myogenesis and somite formation (Bryson-Richardson and Currie, 2008; Dequéant and Pourquié, 2008). However, when we overexpressed *Bmp4*, we observed a significant increase in *Pax7* expression both by RT-PCR and by cell counts after Pax7 immunostaining (mean 17 cells/cap) compared with control (mean 0.22 cells/cap) (see Fig. S3 and Table S4 in the supplementary material). A dose-response study with *Bmp4* mRNA showed that the highest number of Pax7+ cells was achieved at 50 pg of mRNA (Fig. 5). Similar results were achieved by treatment with BMP4 protein (see Fig. S4 in the supplementary material).

Increases in *Pax7* expression and Pax7-positive cells were also observed after overexpression of *Msx1* (mean 27 cells/cap), a known downstream target of BMP signaling (Suzuki et al., 1997), and *Fgf8* (mean 21 cells/cap), which is expressed in the posterior mesoderm surrounding the blastopore in the pre-somite stage embryo (Christen and Slack, 1997).

We next wanted to determine whether we could trigger the formation of Pax7-positive cells in neurula stage paraxial explants, which form virtually no Pax7-positive cells on isolation (Fig. 3), by induction with BMP4. Paraxial explants cultured in normal medium did not develop Pax7-positive cells, whereas with 100 ng/ml BMP4 for 24 hours followed by an additional 3 days in culture they formed a large number (mean=31; Fig. 6). Dorsolateral explants formed similar numbers of Pax7-positive cells with or without the BMP treatment. When paraxial explants were treated with BMP starting at different stages, the increase was only seen when treatment was commenced at stage 13, and not at stage 18 or 22 (Table 2). This shows that competence to form Pax7-positive cells is only present early on and this is consistent with the data on Noggin-induced inhibition (see below), indicating that the BMP-induced specification of satellite cell progenitors occurs during the neurula stages. In this experiment, the 'paraxial' explants from later stages than 13, because they are the same width as at stage 13, contain former dorsolateral tissue which has converged in the intervening period. For this reason, the larger number of Pax7-positive cells in the controls is to be expected.

Effects on satellite cell formation in vivo

We next wanted to determine if the satellite cell inducing factors identified by means of our in vitro assays also regulated their formation in vivo. We co-injected either *Bmp4* (10 pg), *Msx1* (100 pg) or *Fgf8* (100 pg) with *Gfp* (80 pg) mRNA as a lineage tracer into either C3 or C4 blastomeres of a 32-cell stage embryo to fill paraxial or lateral mesoderm of the trunk. Expression domains were verified by observation of GFP expression the next day, and embryos were cultured in 0.1×NAM for 5 days. The tails of tadpoles were then fixed and analyzed for changes in satellite cell number by whole-mount immunofluorescence for Pax7 and muscle Myosin. A standard square was counted for each tadpole, so the

Table 2. Stage dependence of induction of Pax7+ cells by BMP4

	Stage 13	Stage 18	Stage 22
Control	1.4 (±1.14)	16 (±6.5)	21.8 (±4.6)
BMP4	26 (±3.39)	13.6 (±3.36)	21.2 (±4.6)

Explants (100 μm wide) from the paraxial region were dissected at stages 13, 18 or 22 and cultured for 4 days without or with BMP4. Numbers represent the mean number of Pax7-positive cells per explant averaged from five explants per stage (± indicates standard error).

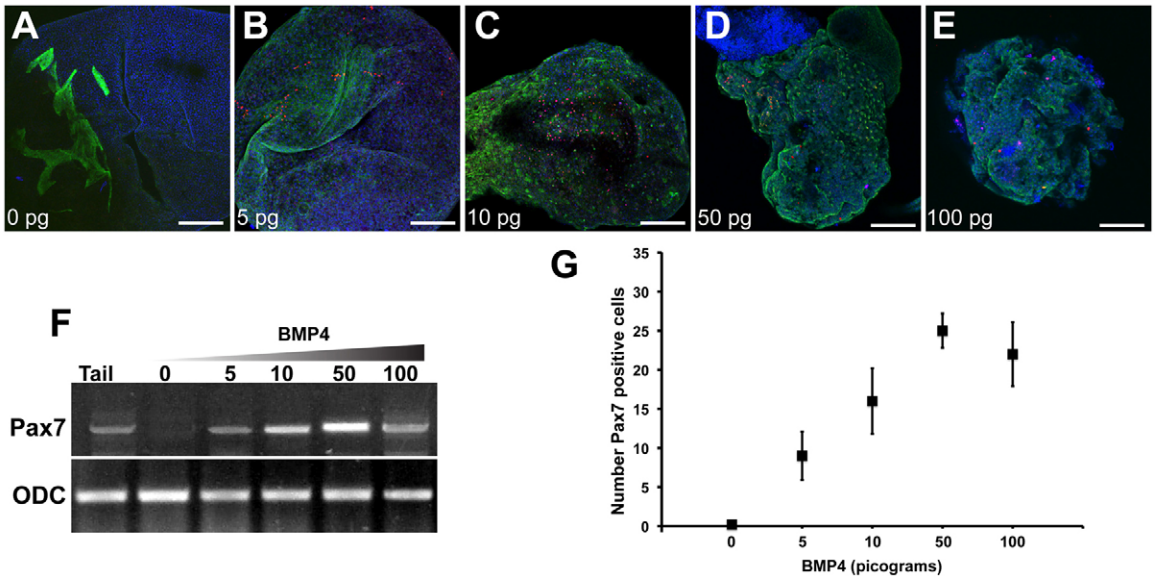

Fig. 5. Pax7-positive cells induced by BMP4 in FGF-treated animal caps. (**A-E**) Immunofluorescence staining of Pax7 (red) and Myosin (green) of animal caps injected with different doses of *Bmp4* mRNA. Scale bars: 200 μm. (**F**) RT-PCR analysis of *Pax7* expression in response to *Bmp4* mRNA. (**G**) Number of Pax7-positive cells counted in animal caps after injection of *Bmp4* mRNA. Five explants were sectioned per treatment for cell counts and three per treatment for RT-PCR analysis. Results are mean ± s.e.m.

figures represent the numbers of Pax7-positive cells within a certain volume of tail muscle, not in the domains filled by C3 or C4 blastomeres. This is why the control figure is similar for both.

In C3-injected embryos we found that *Bmp4* (mean=303), *Msx1* (mean=287) and *Fgf8* (mean=291) all showed significant increases in the number of Pax7-positive cells compared with control (mean=142; Fig. 7). Similarly, overexpression of these factors in lateral plate (C4) increased the number of Pax7-positive cells formed by *Bmp4* (mean=211), *Msx1* (mean=265) and *Fgf8* (mean=223) compared with control (mean=127; Fig. 7). Although overexpression in lateral plate did increase satellite cell formation the percent increase was greater when these factors were overexpressed in paraxial mesoderm. In these cases, the tail muscle morphology was disrupted to varying degrees but the increase in number of satellite cells did not seem to lead to enhanced muscle formation.

Effects of inhibiting the BMP gradient

If satellite cell progenitor formation is controlled by BMP4 in the neurula stage mesoderm, then we should be able to reverse the increase of Pax7-positive cells in paraxial explants by overexpression of Noggin. We overexpressed Noggin by using a heat shock-inducible *Noggin* transgenic line (*HGEM-Noggin*) previously generated in the laboratory (Beck et al., 2006). First, we needed to establish that the induced Noggin is sufficiently active to inhibit concentrations of BMP that will induce the formation of Pax7-positive cells. To do this, we subjected paraxial explants from stage 13/14 *HGEM-Noggin* transgenic embryos to a 15-minute heat shock to induce expression of Noggin. Explants were then maintained in media containing BMP4 for 20 hours and subjected to a second heat shock. They were then transferred to normal medium without BMP4 and cultured for an additional 3 days. As expected from the experiments described above, paraxial explants treated with BMP4 form many Pax7-positive cells (mean=30; Fig. 8C), but following induction of *Noggin* the number of Pax7-positive cells is returned to the control level (mean=0.23; Fig. 8D). This demonstrates that the heat shock induction of *Noggin* in this transgenic line is able to inhibit levels of BMP4 that are required to induce satellite cell formation.

The most critical experiment was then to dissect out dorsolateral explants from neurulae, heat shock to induce *Noggin*, and examine the number of Pax7-positive cells formed (Fig. 8B). This showed a dramatic reduction of numbers of Pax7-positive cells compared to controls (Fig. 8A). This loss of function experiment enables us to conclude that the formation of Pax7-positive cells from the dorsolateral mesoderm is indeed dependent on endogenous BMP signaling. Furthermore, the timing of this experiment indicates that the satellite cell progenitors cannot be determined, i.e. irreversibly committed, before the neurula stage, because the Noggin induction can prevent their formation when administered to explants that are at a stage equivalent to the commencement of neural tube closure. It also confirms that the effects of BMP signaling that we observe are exerted during the period of satellite cell specification, within 24 hours of the open neurula, and not at later stages of myogenesis (3-5 days post-fertilization).

Possible intermediate steps

BMP signaling is mediated by phosphorylation of Smad1 and Smad5, so it is to be predicted that such phosphorylation would be detectable in the dorsolateral mesoderm of the neurula. Accordingly, we immunostained sections of open neural plate embryos with anti-Smad1-phosphate. Some positive nuclei are found in the dorsolateral mesoderm, but not in the paraxial mesoderm (mean 8.8 positive cells/3 sections, *n*=5 embryos; Fig. 9A). This is consistent with an active response to BMP signaling in this region at this time.

We also carried out in situ hybridization for *Msx1*. In common with previously published results, there is clear expression in the neural crest (Fig. 9B). However, on sections there is no visible expression in any part of the mesoderm (Fig. 9C). So although *Msx1* has a potent effect on Pax7-positive cell formation following overexpression, we cannot be sure that it is really an intermediate step in the process in vivo.

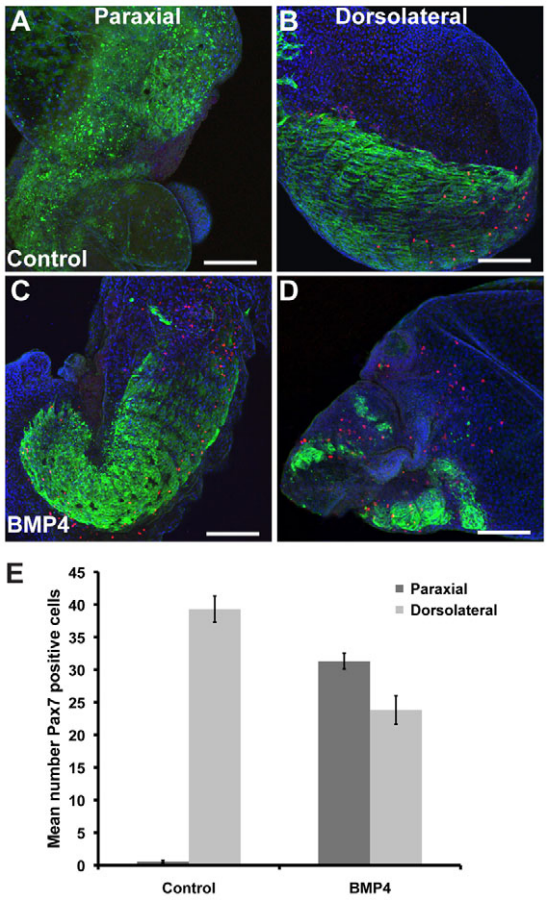

Fig. 6. Regulation of satellite cell formation in neurula stage explants by BMP4. All explants are stained for Myosin (green) and Pax7 (red). (**A**) Paraxial explant. (**B**) Dorsolateral explant. (**C**) Paraxial + BMP4. (**D**) Dorsolateral + BMP4. Scale bars: 200 μm. (**E**) Pax7-positive cells in each type of explant. *n*=5 per group. Results are mean ± s.e.m.

DISCUSSION

Embryonic origin of satellite cells

In the past, the majority view has been that satellite cells originate from the same organ rudiment as produces the skeletal muscle (Armand et al., 1983; Gros et al., 2005; Relaix et al., 2005). A minority has considered that they derive from a completely different site such as the dorsal aorta, other blood vessels or the bone marrow (De Angelis et al., 1999; Gussoni et al., 1999; Seale and Rudnicki, 2000). Our results indicate that neither view is entirely correct. At least in *Xenopus* embryos, the satellite cells arise from a region that is morphologically part of the lateral plate mesoderm at the neurula stage, adjacent to, but distinct from, the main paraxial plate. Some of our experiments show that Pax7-positive cells can arise without accompanying myofibers, indicating that the progenitor cell populations for satellite cells and myofibers must be different.

In the *Xenopus* neurula, the dorsolateral mesoderm is distinct from the paraxial mesoderm in that it is thinner and is located outside the neural folds (Fig. 1). However, it does converge to become incorporated into the somites in the course of dorsal convergence movements in the late neurula and early tailbud stages [see Fig. S2 in the supplementary material and Hamilton (Hamilton, 1969)]. The 'presomite plate' is often considered to be identical to the thick paraxial mesoderm, but if the presomite plate is defined as all cells that later contribute to the somite, it must obviously include some part of the lateral plate. Once they become visible, satellite cells are found throughout the myotomes, so the progenitor cells must migrate as individuals into the central myotome region, which is formed from the paraxial mesoderm. We do not know whether all the cells from a specific dorsolateral level of mesoderm become satellite cells, or whether only some do so with the others becoming muscle fibers or fibroblasts; however, the sparse staining for Smad1-phosphate shown in Fig. 9 suggests that only some cells are responding to BMP at this time. The mouse and chick experiments, indicating an origin from the central dermomyotome, were carried out after somite formation and therefore corresponded to a much later stage in *Xenopus* than our own experiments, perhaps around the equivalent of stage 35. For this reason, we consider that the *Xenopus* data presented here are not necessarily inconsistent with the data from the amniote species. We predict that if it is possible to locate a population of satellite cell precursors in amniotes before somitogenesis then they too are likely to lie in the dorsal lateral plate, and experiments to test this hypothesis are currently in progress.

There has been much recent work on the zebrafish devoted to establishing how various types of muscle cell arise from the somites (Hollway et al., 2007; Stellabotte and Devoto, 2007; Stellabotte et al., 2007). This has shown the existence of a

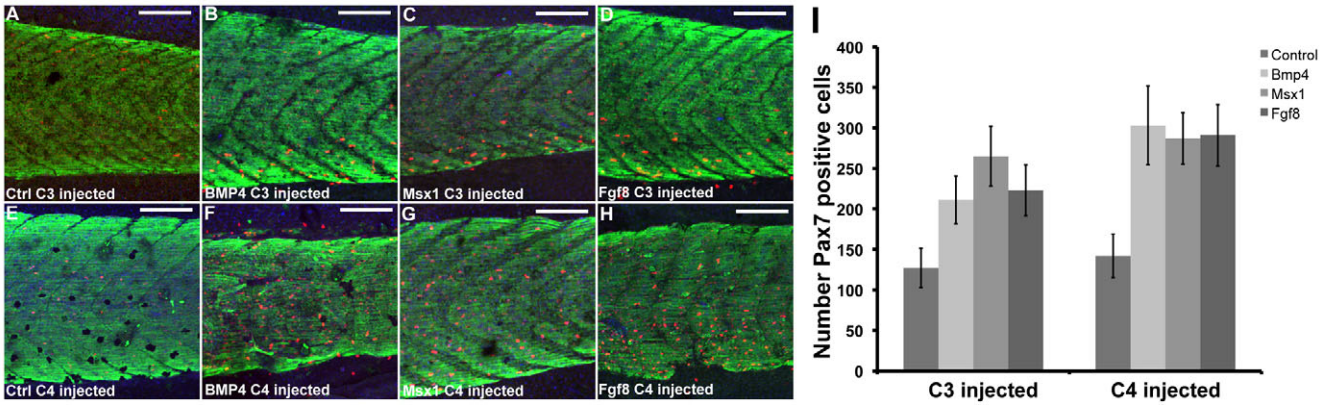

Fig. 7. Effect on satellite cell formation of overexpressing candidate genes in vivo. (**A-H**) Whole mounts of tail muscle of whole tadpoles which had the indicated mRNA injected into C3 or C4 at the three-cell stage. An increase in satellite cell formation is evident for all three genes. Scale bars 200 μm. (**I**) Total number of satellite cells in a standard area of tail muscle, following overexpression of the indicated gene in blastomere C3 or C4. *n*=5 per group. Results are mean ± s.e.m.

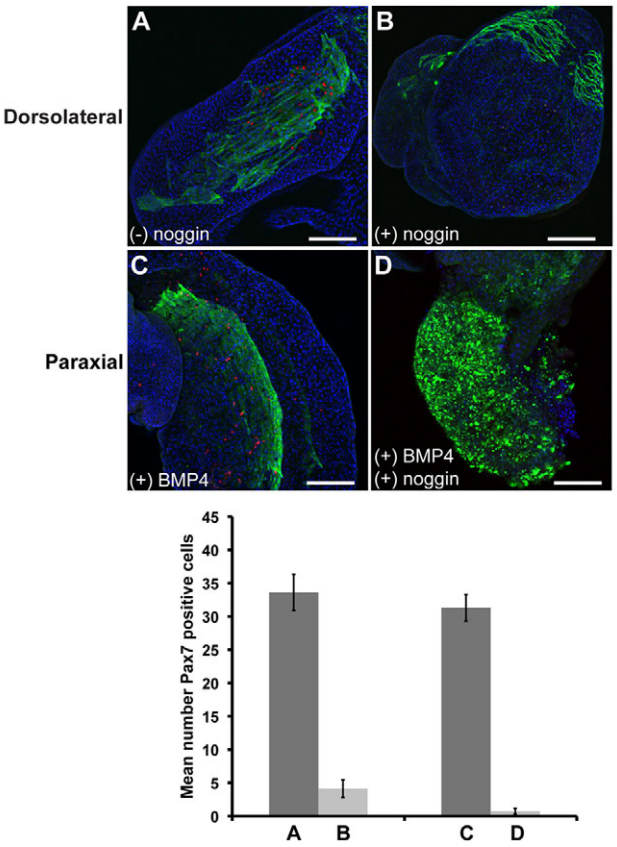

Fig. 8. Suppression of satellite cell formation in neurula stage explants by Noggin. Explants taken from *HGEM-Noggin* embryos at the neurula stage and allowed to develop for 4 days. (+) noggin indicates that the explants received heat shocks to induce *Noggin* expression; (–) noggin indicates that they did not. (**A**) Dorsolateral explant. Like wild-type explants, this forms numerous Pax7-positive cells. (**B**) Dorsolateral explant with induced Noggin forms very few Pax7-positive cells. (**C**,**D**) The induced Noggin is biologically active in the desired range. (C) An unheated paraxial explant treated with BMP4. Like similar wild-type explants, this shows induction of numerous Pax7-positive cells. D shows a paraxial explant that is treated with BMP4 and heated to induce Noggin. In this case, there is no induction of Pax7-positive cells, indicating that the induced Noggin can inhibit BMP4 in the relevant concentration range. Bar chart shows Pax7-positive cell counts for each type of explant. *n*=5 per group. Data are mean ± s.e.m. Scale bars: 200 μm.

population of anterior border cells within each newly formed somite, not expressing myogenic regulatory factors, that migrate to the outer surface of the myotome and form a layer of thin cells that are Pax7 positive. Some of these subsequently enter the myotomes and become satellite cells. Others contribute to myofibers of myotomes, body wall or pectoral fin, or to fibroblast-like cells in the dermis and dorsal fin. This illustrates the principle that satellite cells may arise separately from the main myotomal fiber mass and migrate into it. However, the course of somitogenesis in *Xenopus* is not the same as the zebrafish. Concurrent with segmentation of the somites there is an early rotation of all the prospective myotome cells to an anteroposterior orientation such that each myotome is one cell long (Hamilton, 1969). There is also a layer described as the dermatome, or the dermomyotome, lying outside the myotomes. This is visible in Plate 38 of Hausen's atlas (Hausen and Riebesell, 1991) and has been described by various authors previously (Hamilton, 1969; Blackshaw and Warner, 1976). According to a study by Grimaldi et al. (Grimaldi et al., 2004) this layer is uniformly positive for Pax3. Owing to the difference of cell movements during segmentation, we consider it very unlikely that this layer comes from the anterior of each somite, as seen in the zebrafish. We believe that it arises from the dorsolateral mesoderm as a result of the dorsal convergence movement described by Hamilton. If so, it is likely that the prospective satellite cells are located in this layer before entering the myotomes. However, in *Xenopus* this layer of cells is not uniformly Pax7 positive. In fact there is very little Pax7 expression at all in the tailbud stages (Chen et al., 2006).

Role of Pax7

Pax7 is a transcription factor expressed in muscle satellite cells but not in mature myofibers (Seale et al., 2000). It was initially reported that *Pax7*$^{-}$ mice lacked satellite cells, but was subsequently shown that they did develop satellite cells which were not capable of self-renewal (Oustanina et al., 2004). In *Xenopus*, we showed that *Pax7* was required for regeneration of muscle following tail amputation (Chen et al., 2006), although in mice there remains some dispute about the need for *Pax7* for muscle regeneration (Lepper et al., 2009).

In *Xenopus*, *Pax7* is expressed in the neural crest during the neurula stages. Subsequently, there is a low level expression in somites and myotomes, but no Pax7-positive outer layer as is seen in the zebrafish (Chen et al., 2006). There is extensive expression in neurons forming in the dorsal half of the neural tube and spinal cord. The picture in the mouse and chick is generally similar, although in these amniote species there is a higher and more general expression in the dermomyotome (Lacosta et al., 2005; Horst et al., 2006). In mammals, the related transcription factor Pax3 is expressed in the whole early somite and satellite cell precursors express both Pax3 and Pax7 (Relaix et al., 2005; Buckingham and Relaix, 2007).

As *Pax7*$^{-}$ mutant mice do form satellite cells, *Pax7* must be dispensable for their initial formation in development, even if it required later for self-renewal. But because of the close association with *Pax3*, it is possible that *Pax3* rescues the formation of satellite cells in the absence of *Pax7*. Our own evidence clearly confirms that *Pax7* is not required for satellite cell formation. We show that overexpression of *Pax7* in the presomite plate or in FGF-treated animal caps does not increase satellite cell formation, and that antagonism of Pax7 function with *Pax7EnR* does not reduce satellite cell formation from the dorsolateral mesoderm. We also show that Pax3 does not drive satellite cell formation, or Pax7 expression, in FGF-treated animal caps (see Table S4 in the supplementary material). These collected data make it very unlikely that Pax7 or Pax3 drives the initial specification of satellite cells in development.

Pax7 as a marker

It is legitimate to ask whether it is sufficient to use the expression of Pax7 to identify satellite cells. In our previous publication (Chen et al., 2006), we showed that they corresponded to morphological satellite cells and that they were active in DNA synthesis during tail growth. Many, but not all, of the Pax7-positive cells in muscle also express NCAM, a recognized marker for satellite cells in mouse. In many of the explant experiments reported here, the Pax7-positive cells are separated from muscle fibers. In such circumstances the satellite cells obviously cannot be localized

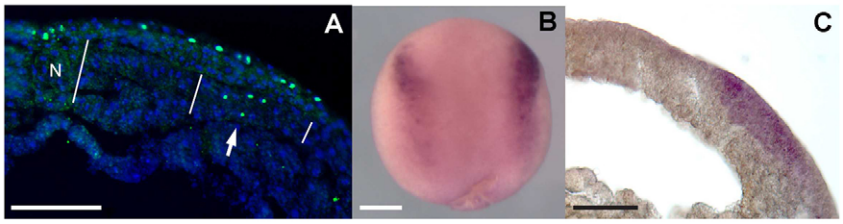

Fig. 9. Smad1-phosphate and *Msx1* expression. (**A**) Immunostain of cryosection of stage 13 neurula showing some nuclei positive for Smad1-P in the dorsolateral mesoderm (arrow), but not the paraxial mesoderm. White lines indicate the approximate extent of the paraxial and dorsolateral explants used in other experiments. N, notochord. (**B**) Whole-mount in situ hybridization of stage 13 neurula for *Msx1*. (**C**) In situ hybridization for *Msx1* on section: staining is apparent only in the neural crest. Scale bars: 100 μm.

under the basement membrane of fibers, which is a major criterion for identification. This is why we refer to 'Pax7-positive cells' rather than 'muscle satellite cells' in the relevant sections. However, we believe that they are in fact satellite cells. The only other Pax7-positive cells in the body during the relevant developmental stages are various classes of neuron in the central nervous system, but none of our experiments generated ectopic neural tissue, and the Pax7-positive cells do not resemble neurons morphologically.

Role of the BMP gradient

The ventral-to-dorsal gradient of BMP was discovered in *Xenopus* and later shown to be a general feature of early vertebrate development (Hemmati-Brivanlou and Thomsen, 1995; Yamagishi et al., 1995; Jones et al., 1996; Dosch et al., 1997; Kurata et al., 2001; De Robertis, 2009). BMPs become activated autonomously due to maternal BMP activity activating their own genes' transcription. The expression domains are later refined by negative interactions that ensure that cells cannot at the same time express BMP genes and organizer genes (Reversade and De Robertis, 2005). The gradient depends on diffusion of BMP protein from the producing zone, coupled with inhibition due to binding of Chordin and Noggin from the organizer. The activity of signaling is converted into a nuclear level of phosphorylated Smad-1 and -5 (Simeonia and Gurdon, 2007). Many genes are activated by BMP signaling, and an obvious candidate to be in the satellite cell formation pathway was *Msx1* (Suzuki et al., 1997; Maeda et al., 1997). We find that that *Msx1* behaves very similarly to BMP in our assays of Pax7-positive cell formation. However, we do not find that it is expressed in the dorsolateral mesoderm of the neurula, so unless it is active at sub-detection levels, we conclude that it is not involved in satellite cell formation in normal development. A similar consideration may apply to FGF8. This is expressed in the posterior of the forming axis and has been considered a posteriorizing factor in other vertebrates as well as in *Xenopus* (Christen and Slack, 1997; Dubrulle and Pourquie, 2004). The role of FGF8 has been investigated in zebrafish myogenesis and has a negative effect on the formation of Pax7-positive cells, albeit these are cells of the dermomyotome layer rather than the definitive satellite cells (Hammond et al., 2007).

Timing of satellite cell specification

We believe that satellite cell specification is occurring during neurula stages rather than the tadpole stages for two reasons. First, the effect of BMP treatment on paraxial explants is most pronounced when the BMP is added from stage 13, rather than from stage 18 or later (Table 2). This means that competence to respond to BMP is present in the open neurula and falls away by neural tube closure. Second, satellite cell formation in dorsolateral explants from *HGEM-Noggin* neurulae is suppressed by heat shock The *Noggin* mRNA induced by heat shock decays after about 24 hours (Beck et al., 2006) so this inhibitory effect cannot still be persisting during the tadpole stages when the Pax7 expression actually becomes visible.

The BMP gradient is normally supposed to be a phenomenon of the gastrula, as this is when neural induction and mesoderm dorsalization take place (Lettice and Slack, 1993). But we also know of studies indicating some lability of mesoderm explanted from the neurula of urodele embryos (Yamada, 1937; Forman and Slack, 1980). So it does seem likely that the BMP gradient can remain active through the neurula stages and participate in additional dorsoventral decisions, such as the formation of the satellite cell precursor zone.

Very recently, two other studies have investigated the effects of BMP signaling on satellite cell numbers, although in rather different contexts from our own work. This effect is in the same direction as that which we have described, although at a much later stage of development, when satellite cells are already present in the muscles. In the first study it was shown that additional BMP signaling in the limbs of late chick embryos can stimulate satellite cell number, while Noggin will reduce it (Wang et al., 2010). In the second study, focusing on the myotomes of zebrafish embryos, it was shown that upregulation of BMP delays the differentiation of the Pax7-positive dermomyotome cells to myofibers leading to a temporary increase in Pax7-positive cell numbers (Patterson et al., 2010). Although these works describe processes leading in the same direction as ours, we feel that the events concerned are later in development that the satellite cell precursor specification that we describe. In our experiments, the effects of BMP signaling are exerted at neurula stage when there are no Pax7-positive cells present, and the satellite cells themselves differentiate several days later.

In summary, our work demonstrates an origin for muscle satellite cells from the dorsolateral mesoderm and a dependence of their formation on the BMP gradient in the early embryo. We consider that this mechanism is quite likely also to exist in higher vertebrates.

Acknowledgements

This work was supported by a NIH (NIAMS) Training Grant #T32-AR050938, NIH (NIGMS) R01 grant #R01GM088500 and Wellcome Trust Programme Grant #60082. Deposited in PMC for release after 6 months.

Competing interests statement

The authors declare no competing financial interests.

Supplementary material

Supplementary material for this article is available at
http://dev.biologists.org/lookup/suppl/doi:10.1242/dev.056481/-/DC1

References

Armand, O., Boutineau, A., Mauger, A., Pautou, M. and Kieny, M. (1983). Origin of satellite cells in avian skeletal muscles. *Arch. Anat. Microsc. Morphol. Exp.* **72**, 163-181.

Beck, C. W., Christen, B., Barker, D. and Slack, J. M. W. (2006). Temporal requirement for bone morphogenetic proteins in regeneration of the tail and limb of Xenopus tadpoles. *Mech. Dev.* **123**, 674-688.

Blackshaw, S. E. and Warner, A. E. (1976). Low resistance junctions between mesoderm cells during development of trunk muscles. *J. Physiol.* **255**, 209-230.

Bryson-Richardson, R. J. and Currie, P. D. (2008). The genetics of vertebrate myogenesis. *Nat. Rev. Genet.* **9**, 632-646.

Buckingham, M. and Relaix, F. (2007). The role of pax genes in the development of tissues and organs: Pax3 and Pax7 regulate muscle progenitor cell functions. *Annu. Rev. Cell Dev. Biol.* **23**, 645-673.

Chargé, S. B. and Rudnicki, M. A. (2004). Cellular and molecular regulation of muscle regeneration. *Physiol. Rev.* **84**, 209-238.

Chen, Y., Lin, G. F. and Slack, J. M. W. (2006). Control of muscle regeneration in the Xenopus tadpole tail by Pax7. *Development* **133**, 2303-2313.

Christen, B. and Slack, J. M. W. (1997). FGF-8 is associated with anteroposterior patterning and limb regeneration in Xenopus. *Dev. Biol.* **192**, 455-466.

Dale, L. and Slack, J. M. W. (1987). Fate map for the 32 cell stage of *Xenopus laevis*. *Development* **99**, 527-551.

Daughters, R. S., Hofbauer, R. D., Grossman, A. W., Marshall, A. M., Brown, E. M., Hartman, B. K. and Faris, P. L. (2001). Ondansetron attenuates CCK induced satiety and c-fos labeling in the dorsal medulla. *Peptides* **22**, 1331-1338.

De Angelis, L., Berghella, L., Coletta, M., Lattanzi, L., Zanchi, M., Cusella-De Angelis, M. G., Ponzetto, C. and Cossu, G. (1999). Skeletal myogenic progenitors originating from embryonic dorsal aorta coexpress endothelial and myogenic markers and contribute to postnatal muscle growth and regeneration. *J. Cell Biol.* **147**, 869-877.

De Robertis, E. M. (2009). Spemann's organizer and the self-regulation of embryonic fields. *Mech. Dev.* **126**, 925-941.

Dequéant, M.-L. and Pourquié, O. (2008). Segmental patterning of the vertebrate embryonic axis. *Nat. Rev. Genet.* **9**, 370-382.

Dosch, R., Gawantka, V., Delius, H., Blumenstock, C. and Niehrs, C. (1997). BMP-4 acts as a morphogen in dorsoventral mesoderm patterning in Xenopus. *Development* **124**, 2325-2334.

Dubrulle, J. and Pourquie, O. (2004). fgf8 mRNA decay establishes a gradient that couples axial elongation to patterning in the vertebrate embryo. *Nature* **427**, 419-422.

Forman, D. and Slack, J. M. W. (1980). Determination and cellular commitment in the embryonic amphibian mesoderm. *Nature* **286**, 492-494.

Gargioli, C. and Slack, J. M. W. (2004). Cell lineage tracing during Xenopus tail regeneration. *Development* **131**, 2669-2679.

Grimaldi, A., Tettamanti, G., Martin, B. L., Gaffield, W., Pownall, M. E. and Hughes, S. M. (2004). Hedgehog regulation of superficial slow muscle fibres in Xenopus and the evolution of tetrapod trunk myogenesis. *Development* **131**, 3249-3262.

Gros, J., Manceau, M., Thome, V. and Marcelle, C. (2005). A common somitic origin for embryonic muscle progenitors and satellite cells. *Nature* **435**, 954-958.

Gussoni, E., Soneoka, Y., Strickland, C. D., Buzney, E. A., Khan, M. K., Flint, A. F., Kunkel, L. M. and Mulligan, R. C. (1999). Dystrophin expression in the mdx mouse restored by stem cell transplantation. *Nature* **401**, 390-394.

Hamilton, L. (1969). The formation of somites in Xenopus. *J. Embryol. Exp. Morphol.* **22**, 253-264.

Hammond, C., Hinits, Y., Osborn, D., Minchin, J., Tettamanti, G. and Hughes, S. (2007). Signals and myogenic regulatory factors restrict pax3 and pax7 expression to dermomyotome-like tissue in zebrafish. *Dev. Biol.* **302**, 504-521.

Hausen, P. and Riebesell, M. (1991). *The Early Development of Xenopus laevis*: Berlin: Springer-Verlag.

Hawke, T. J. and Garry, D. J. (2001). Myogenic satellite cells: physiology to molecular biology. *J. Appl. Physiol.* **91**, 534-551.

Hemmati-Brivanlou, A. and Thomsen, G. H. (1995). Ventral mesodermal patterning in Xenopus embryos: Expression patterns and activities of BMP-2 and BMP-4. *Dev. Genet.* **17**, 78-89.

Hollway, G. E., Bryson-Richardson, R. J., Berger, S., Cole, N. J., Hall, T. E. and Currie, P. D. (2007). Whole-somite rotation generates muscle progenitor cell compartments in the developing zebrafish embryo. *Dev. Cell* **12**, 207-219.

Horst, D., Ustanina, S., Sergi, C., Mikuz, G., Juergens, H., Braun, T. and Vorobyov, E. (2006). Comparative expression analysis of Pax3 and Pax7 during mouse myogenesis. *Int. J. Dev. Biol.* **50**, 47-54.

Isaacs, H. V., Pownall, M. E. and Slack, J. M. W. (1994). eFGF regulates Xbra expression during Xenopus gastrulation. *EMBO J.* **13**, 4469-4481.

Jones, C. M., Dale, L., Hogan, B. L. M., Wright, C. V. E. and Smith, J. C. (1996). Bone morphogenetic protein-4 (BMP-4) acts during gastrula stages to cause ventralization of Xenopus embryos. *Development* **122**, 1545-1554.

Kuang, S., Gillespie, M. A. and Rudnicki, M. A. (2008). Niche regulation of muscle satellite cell self-renewal and differentiation. *Cell Stem Cell* **2**, 22-31.

Kurata, T., Nakabayashi, J., Yamamoto, T. S., Mochii, M. and Ueno, N. (2001). Visualization of endogenous BMP signaling during Xenopus development. *Differentiation* **67**, 33-40.

Lacosta, A. M., Muniesa, P., Ruberte, J., Sarasa, M. and Dominguez, L. (2005). Novel expression patterns of Pax3/Pax7 in early trunk neural crest and its melanocyte and non-melanocyte lineages in amniote embryos. *Pigment Cell Res.* **18**, 243-251.

Lepper, C., Conway, S. J. and Fan, C. M. (2009). Adult satellite cells and embryonic muscle progenitors have distinct genetic requirements. *Nature* **460**, 627-631.

Lettice, L. A. and Slack, J. M. W. (1993). Properties of the dorsalizing signal in gastrulae of Xenopus laevis. *Development* **117**, 263-272.

Maeda, R., Kobayashi, A., Sekine, R., Lin, J.-J., Kung, H. and Maéno, M. (1997). Xmsx-1 modifies mesodermal tissue pattern along dorsoventral axis in Xenopus laevis embryo. *Development* **124**, 2553-2560.

Mauro, A. (1961). Satellite cells of skeletal muscle fibres. *J. Biophys. Biochem. Cytol.* **9**, 493-498.

Morgan, J. E. and Partridge, T. A. (2003). Muscle satellite cells. *Int. J. Biochem. Cell Biol.* **35**, 1151-1156.

Morrison, J. I., Loof, S., He, P. and Simon, A. (2006). Salamander limb regeneration involves the activation of a multipotent skeletal muscle satellite cell population. *J. Cell Biol.* **172**, 433-440.

Oustanina, S., Hause, G. and Braun, T. (2004). Pax7 directs postnatal renewal and propagation of myogenic satellite cells but not their specification. *EMBO J.* **23**, 3430-3439.

Patterson, S. E., Bird, N. C. and Devoto, S. H. (2010). BMP regulation of myogenesis in zebrafish. *Dev. Dyn.* **239**, 806-817.

Pollet, N., Muncke, N., Verbeek, B., Li, Y., Fenger, U., Delius, H. and Niehrs, C. (2005). An atlas of differential gene expression during early Xenopus embryogenesis. *Mech. Dev.* **122**, 365-439.

Relaix, F., Rocancourt, D., Mansouri, A. and Buckingham, M. (2005). A Pax3/Pax7-dependent population of skeletal muscle progenitor cells. *Nature* **435**, 948-953.

Reversade, B. and De Robertis, E. M. (2005). Regulation of ADMP and BMP2/4/7 at opposite embryonic poles generates a self-regulating morphogenetic field. *Cell* **123**, 1147-1160.

Seale, P. and Rudnicki, M. A. (2000). A new look at the origin, function, and "stem cells" status of muscle satellite cells. *Dev. Biol.* **218**, 115-124.

Seale, P., Sabourin, L. A., Girgis-Gabardo, A., Mansouri, A., Gruss, P. and Rudnicki, M. A. (2000). Pax7 is required for the specification of myogenic satellite cells. *Cell* **102**, 777-786.

Simeonia, I. and Gurdon, J. B. (2007). Interpretation of BMP signaling in early Xenopus development. *Dev. Biol.* **308**, 82-92.

Slack, J. M. W., Darlington, B. G., Heath, J. K. and Godsave, S. F. (1987). Mesoderm induction in early Xenopus embryos by heparin-binding growth factors. *Nature* **326**, 197-200.

Stellabotte, F. and Devoto, S. H. (2007). The teleost dermomyotome. *Dev. Dyn.* **236**, 2432-2443.

Stellabotte, F., Dobbs-McAuliffe, B., Fernandez, D. A., Feng, X. and Devoto, S. H. (2007). Dynamic somite cell rearrangements lead to distinct waves of myotome growth. *Development* **134**, 1253-1257.

Suzuki, A., Ueno, N. and Hemmati-Brivanlou, A. (1997). Xenopus msx1 mediates epidermal induction and neural inhibition by BMP4. *Development* **124**, 3037-3044.

Tucker, A. S. and Slack, J. M. W. (1995). The Xenopus laevis tail-forming region. *Development* **121**, 249-262.

Wang, H., Noulet, F., Edom-Vovard, F., Le Grand, F. and Duprez, D. (2010). Bmp signaling at the tips of skeletal muscles regulates the number of fetal muscle progenitors and satellite cells during development. *Dev. Cell* **18**, 643-654.

Yamada, T. (1937). Das determinationzustand des Rumpfmesoderms im Molchkeim nach der Gastruatlion. *Wilhelm Roux's Arch. Entw. Mech. Orgs.* **137**, 151-270.

Yamagishi, T., Nishimatsu, S. I., Nomura, S., Asashima, M., Murakami, K. and Ueno, N. (1995). Expression of Bmp-2,4 genes during early development in Xenopus. *Zool. Sci.* **12**, 355-358.

Table S1. PCR primers

Gene	Temperature (°C)	Forward primer	Reverse primer
Pax7	57	5′-TCAATAATGGTCTCTCCCCGC-3′	5′-TTGCCAGGTAATCAACAGCGG-3′
Pax3	57	5′-ATTCAACCACCTGATTCCAGG-3	5′-GCCTGTGAACTGTGTTGCTTG-3′
Myf5	52	5′-CTATTCAGAATGGAGATGGT-3′	5′-GTCTTGGAGACTCTCAATA-3′
MyoD	58	5′-ACATGGAAGTCATGAGGGAT-3′	5′-AAGAGTCACGTGCACCAGCCT-3′
Odc	55	5′-ACACGGCATTGATCCTACAG-3′	5′-AGCTCCTTCGGTGTAATGAC-3′

Table S2. Distribution of RDA after 32-cell stage injection

		Stage 16				
RDA injection site	*n*	Paraxial labeling	Paraxial and dorsolateral	Dorsolateral	Dorsolateral and ventral	Ventral
C3	56	47(84.0%)	9 (16.0%)	0	0	0
C4	50	0	0	34 (68.0%)	16 (32.0%)	0

		Stage 32			
RDA injection site	*n*	Dorsal and middle somite	Middle somite only	Dorsalmost and ventral somite	Ventral somite only
C3	43	43 (100%)	0	0	0
C4	30	0	0	20 (66.7%)	10 (33.3%)

Table S3. Ectopic gene expression induced by *Pax7* mRNA injection at 32-cell stage

	***Pax7* mRNA C3 injection**			***Pax7* mRNA C4 injection**		
	Myf5	*MyoD*	*Pax3*	*Myf5*	*MyoD*	*Pax3*
Stage 16	23 (88.5%)	0	20 (87.0%)	0	0	18 (72%)
Stage 32	35 (87.5%)	0	31 (88.6%)	0	0	17 (65.4%)

Table S4. Candidate factors affecting satellite cell formation

Constructs	Pax7 expression
Bmp4	+++
Msx1	+++
Fgf8	+++
Tbx6	+
Myf5	–
Pax7	–
Pax3	–
Wnt8	–
Wnt3a	–
GSK3B	–
Notch1	–
NICD	–

Candidate factor mRNA (100 pg) was injected into both blastomeres of two-cell stage embryo. Animal caps were collected at stage 8-9, induced with FGF2 and cultured for 5 days. (+) or (–) refers to the expression level of *Pax7* by RT-PCR compared with control caps.